Insect science

Insect Science (2017) 24, 17–26, DOI 10.1111/1744-7917.12285

ORIGINAL ARTICLE

Oxidation resistance 1 (OXR1) participates in silkworm defense against bacterial infection through the JNK pathway

Li-De Su[1], Qiao-Ling Zhang[1] and Zhiqiang Lu[1,2]

[1]*Department of Entomology, College of Plant Protection and* [2]*Key Laboratory of Plant Protection Resources and Pest Management, Ministry of Education, Northwest A&F University, Yangling, Shaanxi 712100, China*

Abstract Bacterial infection causes enhanced reactive oxygen species (ROS) levels in insects. Oxidation resistance 1 (OXR1) plays an antioxidant role in eukaryotic organisms, including insects. In this report, we demonstrated that *Pseudomonas aeruginosa* and *Staphylococcus aureus* infection and hydrogen peroxide (H_2O_2) injection induced the expression of specific transcriptional isoforms of *OXR1* in larval silkworms. We further showed that a Jun kinase (JNK) pathway inhibitor, SP600125, down-regulated expression of *OXR1* during infection, leading to elevated H_2O_2 levels in the hemolymph, resulting in lower viability of the injected bacteria inside the silkworm larvae. Our study suggests that OXR1 participates in protecting larval silkworms from oxidative stress and bacterial infection through the JNK pathway.

Key words *Bombyx mori*; infection; Jun kinase pathway; oxidation resistance 1; reactive oxygen species

Introduction

Reactive oxygen species (ROS) are used to eliminate invading pathogens and parasites in insects (Nappi & Ottaviani, 2000). Knockdown of *dDuox*, which is responsible for hydrogen peroxide (H_2O_2) generation in the *Drosophila* midgut, increased susceptibility of adult flies to infection by bacterial *Erwinia carotovora carotovora 15* (Ha *et al.*, 2005). In the mosquito *Aedes aegypti*, H_2O_2 controls bacterial proliferation in the midgut (Oliveira *et al.*, 2011). H_2O_2 concentration increased in the sand fly midgut after feeding on the insect pathogen *Serratia marcescens*, and feeding of the exogenous ROS scavenger uric acid reduced survival after oral infection with *S. marcescens* (Diaz-Albiter *et al.*, 2011). Oral administration of H_2O_2 as well as silencing of the catalase gene that breaks down H_2O_2 decreased the parasite *Leishmania mexicana* population in the sand fly midgut (Diaz-Albiter *et al.*, 2011, 2012). It was also suggested that a higher level of H_2O_2 in the hemolymph of larval tiger moths, *Parasemia plantaginis*, may provide protection to the host insect from recurring infection by *S. marcescens* (Mikonranta *et al.*, 2014).

Oxidation resistance 1 (*OXR1*) is an evolutionarily conserved gene present in eukaryotic organisms ranging from yeasts to humans. The OXR1 protein family commonly contains a highly conserved TLDc domain at the carboxyl-terminus and a peptidoglycan-binding domain (LysM) at the amino-terminus. Yeast and human oxr1 genes are induced by heat and oxidative stress to protect cells from stress (Elliott & Volkert, 2004). Human *OXR1* is able to suppress oxidative DNA damage, reducing spontaneous mutagenesis in *Escherichia coli* oxidative repair-deficient mutants (Volkert *et al.*, 2000). A recent study showed that human *OXR1* prevents intracellular H_2O_2-induced oxidative stress and maintains mitochondrial DNA integrity via the p21 signaling pathway (Yang *et al.*, 2014). OXR1 also plays a critical role as an antioxidant modulator of pathogenesis and disease progression in neurodegenerative disorders (Oliver *et al.*, 2011; Liu *et al.*, 2015). In the nematode *Caenorhabditis elegans*, LMD-3, the homolog of human *OXR1*, participates in the regulation of

Correspondence: Zhiqiang Lu, Department of Entomology, College of Plant Protection, Northwest A&F University, Yangling, Shaanxi 712100, China. Tel: +86 29 8709 1997; email: zhiqiang.lu@nwsuaf.edu.cn

aging through prevention of oxidative stress (Sanada *et al.*, 2014).

Drosophila OXR1 (CG32464, also known as *L82* or mustard) has 24 different transcripts generated by alternative splicing of different exons. Depletion of the *OXR1* locus results in the failure of adult flies to eclose, suggesting an essential role in development (Stowers *et al.*, 1999). In a genetic screening, the OXR1 mutant was found to resemble immune-deficiency (IMD) pathway mutants when flies were orally infected by the Gram-negative bacterium *Vibrio cholerae*. The expression levels of an antimicrobial peptide *Diptericin*, which is regulated directly through the IMD pathway, were dramatically reduced in the *OXR1* mutants under both uninfected and infected conditions. This implies that *OXR1* may modulate IMD signaling by an unknown mechanism (Wang *et al.*, 2012). *OXR1* mutants are resistant to oral *V. cholerae* infection and maintain higher rates of intestinal stem cell division during *V. cholerae* infection, suggesting that *OXR1* is also involved in the regulation of epithelial regeneration (Wang *et al.*, 2013). In the mosquito *Anopheles gambiae*, silencing of *OXR1* resulted in a significant decrease in the parasite *Plasmodium berghei* load (Brandt *et al.*, 2008). Further study revealed that the Jun kinase (JNK) pathway regulates *OXR1* expression and subsequently regulates expression of ROS-detoxifying enzymes, such as catalase and glutathione peroxidase, in mosquito (Jaramillo-Gutierrez *et al.*, 2010).

OXR1 is expressed differentially in *Bombyx mori* diapause eggs and non-diapause eggs. However, RNA interference indicated that *OXR1* is not essential for diapause initiation and/or maintenance (Kobayashi *et al.*, 2014). Overexpression of *BmOXR1* in *Drosophila melanogaster* suggested that it might function as an antioxidant regulator in the silkworm (Kobayashi *et al.*, 2014). In this study, we investigated the participation of *BmOXR1* in silkworm responses to bacterial infection and oxidative stress. Using a specific JNK inhibitor, we also revealed that the JNK pathway regulates *BmOXR1* expression during bacterial infection and oxidative stress.

Materials and methods

Insect rearing and nucleic acid preparation

The silkworm *B. mori* (*Nistari* strain) was reared on mulberry leaves at 27°C under 70% relative humidity and a 12-h light : 12-h dark photoperiod. The fat body was collected by dissecting ice-anesthetized larval silkworms in sterilized physiological saline. Total RNA was extracted from the fat bodies using Tripure reagent (Roche, Basel, Switzerland) according to the manufacturer's instructions. The isolated RNA was purified using the Direct-zol RNA MiniPrep Kit (Zymo Research, Irvine, CA, USA) and used as template for first-strand complementary DNA (cDNA) synthesis using the First-Strand cDNA Synthesis Kit (Roche) following the manufacturer's protocol.

Table 1 Primer sequences used for reverse-transcriptional polymerase chain reaction.

Primer	Sequence
P1	5′- ATCGTGGTGGAACGTGTTTG -3′
P2	5′- CCGGGAAAGATGAACTGT -3′
P3	5′- TCCGACGAAATTTACCGAAC -3′
RP49_F	5′- CCTGTTTACAGGCCGACAAT -3′
RP49_R	5′- GGAATCCATTTGGGAGCATA -3′

Semi-quantitative reverse-transcription polymerase chain reaction

Semi-quantitative reverse-transcription polymerase chain reaction (RT-PCR) was used to determine the *BmOXR1* messenger RNA (mRNA) levels in the fat bodies from different groups of silkworm larvae. PCR conditions were as follows: one cycle at 94°C for 3 min; 30–40 cycles at 94°C for 30 s, 50°C for 45 s, 72°C for 40 s; one cycle of 72°C for 5 min. The *B. mori ribosomal protein 49* (*RP49*) gene was used to standardize mRNA levels. The primers used are listed in Table 1. The PCR products were separated on a 1.5% agarose gel by electrophoresis and visualized by ethidium bromide staining in a BioDoc-It Imaging System (UVP, Upland, CA, USA). PCR products were recovered from the gels using a Gel Extraction Kit (Omega, Norcross, GA, USA) and sent to Sunny Biotechnology (Shanghai, China) for sequencing.

Injection of bacteria and H_2O_2 in silkworms

Pseudomonas aeruginosa (PAO1) and *Staphylococcus aureus* (NCTC 8325) were cultured in Luria-Bertani (LB) broth at 37°C to an optical density (OD) at 600 nm of 0.6–0.8. The bacterial cells were harvested by centrifugation at 8000 × *g* for 15 min, washed three times with 0.85% NaCl and then suspended in saline at 1×10^7 colony-formating units (CFU)/mL. Day 3, fifth instar larvae were injected with *S. aureus* and *P. aeruginosa* preparations at a dosage of 50 μL/larva. Fat bodies were collected from 8–10 larvae at 4, 8 and 24 h post-injection and pooled for RNA preparations.

Fifty microliters of freshly prepared H_2O_2 solution (100, 500 and 2500 μmol/L) were injected into the hemocoel of day 3, fifth instar larvae. Eight to ten larvae were dissected to collect fat bodies for RNA preparation at 3, 6, 12 and 24 h post-injection.

Administration of JNK inhibitor

The JNK pharmacologic inhibitor SP600125 (Santa Cruz Biotechnology Inc., Dallas, TX, USA) was dissolved in DTN buffer (10% dimethyl sulfoxide, 1.5% Tween-20 and 0.85% NaCl). To assess the effect of the JNK inhibitor on *BmOXR1* expression induced by H_2O_2, 50 μL SP600125 (1 mmol/L) were injected into the hemocoel of day 3, fifth instar larvae, and 50 μL of 500 μmol/L H_2O_2 were injected a half hour later. Fat bodies from 8–10 larvae were pooled for RNA preparation at 3, 6, 12 and 24 h post-injection.

To investigate the effect of the JNK inhibitor during bacterial infection, 50 μL of 1 mmol/L SP600125 were injected into the body of day 2, fifth instar larval silkworms. A half hour later, 50 μL of *S. aureus* and *P. aeruginosa* preparations (1×10^7 CFU/mL) or sterilized saline were injected into the body. Silkworm survival was recorded after bacterial infection. Eight hours after infection, five larvae were anesthetized on ice, and hemolymph was collected in an ice-cold Eppendorf tube containing 1.5 μL propylthiouracil. The hemolymph samples were centrifuged at 500 $\times$ *g* for 10 min, and the plasma was used for H_2O_2 concentration assays (see below). Fat bodies were collected from 8–10 larvae at 4, 8, 24 and 48 h post-bacterial infection and saved for RNA preparation. At 24, 48 and 72 h post-infection, hemolymph was also collected for bacterial CFU assays (see below).

Hemolymph H_2O_2 concentration assays

The plasma samples collected at 8 h post-infection were transferred to Amicon Ultra 10K filters (EMD Millipore, Billerica, MA, USA) and centrifuged at 13 000 $\times$ *g* for 5 min. H_2O_2 concentrations in the flow-through were measured using the Amplex Red Hydrogen Peroxide/Peroxidase Assay Kit (Invitrogen, Grand Island, NY, USA). The fluorescence intensity was detected at an excitation/emission of 550 nm/590 nm using a fluorescence microplate reader (Tecan, Männedorf, Switzerland).

CFU counts

After injection with SP600125 and bacterial preparations, five larvae were sacrificed for individual hemolymph collection at 24, 48 and 72 h post-injection. The hemolymph samples were diluted five-fold with sterilized phosphate-buffered saline, and 100 μL were plated on a LB agar plate. The plates were incubated at 37°C for 24 h, and the numbers of colonies growing on the plates were counted.

Evaluation of bacterial sensitivity to H_2O_2

Overnight cultures of *S. aureus* and *P. aeruginosa* were diluted 50-fold in fresh LB medium and grown to an OD_{600} of approximately 0.6–0.8. Different concentrations of H_2O_2 were added to the cultures, and incubation was continued at 37°C with shaking in the dark. The OD_{600} values of the cultures were measured and recorded every 2 h.

Survival analysis

A group of 20 larvae was used to monitor silkworm mortality after bacterial infection as described above. The numbers of surviving larvae were recorded daily. The survival curves were analyzed using the log-rank survival test in GraphPad Prism 5.

Statistical analysis

Student's *t*-test was used to compare H_2O_2 levels and CFUs between the controls and treated samples at each time point. Survival data were analyzed using the log-rank test. Differences of $P < 0.05$, 0.01 and 0.001 are represented as *, ** and ***, respectively.

Results

BmOXR1 gene structure and phylogenetic analysis

We searched for OXR1 homologs in the *B. mori* database using the *D. melanogaster* OXR1 protein sequence (accession number: Q9VNA1) as the query and obtained three cDNA sequences showing high similarity to fly OXR1. These three sequences are AK387280, NM_001145655 and AK383272, which we designated as variants A, B and C, respectively. NM_001145655 has been cloned and characterized recently (Kobayashi *et al.*, 2014). The structures of these genes are illustrated in Figure 1. AK387280 is composed of 24 exons and the start codon ATG is located in exon 2. Exon 3 is missing in NM_001145655. AK383272 is composed of 22 exons with both exons 1 and 3 missing, and the start codon ATG is at the boundary between exons 2 and 4. After PCR

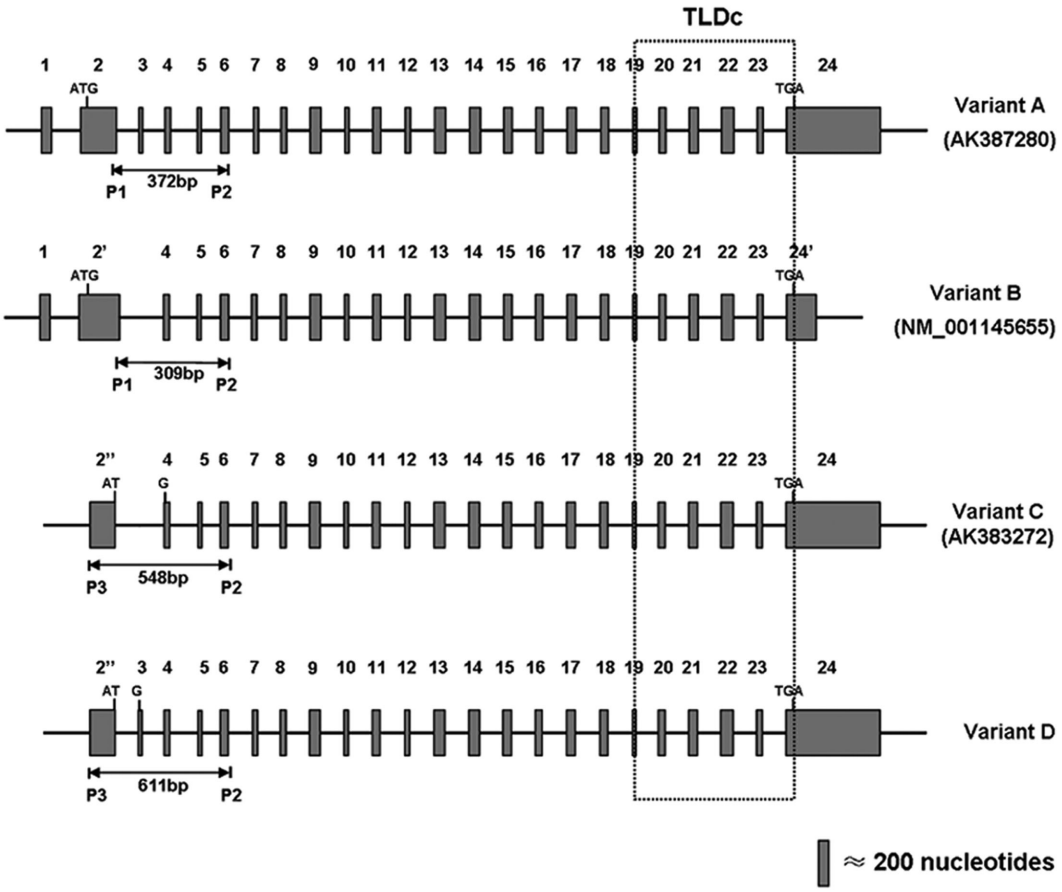

Fig. 1 Genomic organization of splice variants of *BmOXR1* gene. The numbers above the boxes represent exon numbers. The widths of the boxes are proportional to the lengths of exons. The start codon "ATG" and stop codon "TGA" are marked. The TLDc domain is boxed with broken lines. Positions of the primers used in reverse-transcriptional polymerase chain reaction (PCR) for detection of different variants are shown and the PCR product lengths are given.

amplification using specific primers (see Fig. 1 and Table 1), we obtained the expected fragments from these three transcripts and confirmed by sequencing (Fig. 3 and Fig. S1). In addition to the expected amplicons, we obtained a fragment of over 600 bp (Fig. 3). Sequencing of this fragment revealed a transcript containing exon 3, with the start codon ATG at the boundary between exons 2 and 3. We designated this novel transcript as variant D.

The TLDc domain is coded by exons 19–24, which is indicated by a box in Figure 1. The TLDc domain is present in all eukaryotes and highly conserved among species (Blaise *et al.*, 2012). We compared the TLDc domain protein sequences of OXR1 among insects, nematode, mouse, human and yeast and found high similarity among the different species (Fig. 2A). Phylogenetic analysis based on TLDc domain sequence alignment revealed that TLDc from insects form a group (Fig. 2B).

BmOXR1 expression is induced by bacterial infection and H_2O_2

To investigate its role in silkworm immune response, we examined *BmOXR1* transcriptional levels after bacterial infection. Using specific primers and sequence confirmation, we were able to detect different transcripts derived from alternative splicing. As shown in Figure 3A, during the early stages of infection (4 h post-infection), variants C and B were induced strongly by *S. aureus* and *P. aeruginosa* infection. Variant B mRNA maintained a higher level in *P. aeruginosa*- compared with *S. aureus*-infected larvae. In the *S. aureus*-infected larvae, variant D was induced remarkably at 8 hpi (hours post-infection), and variant A was up-regulated at 8 and 24 hpi. This result revealed a complex expression profile for *BmOXR1* upon bacterial infection.

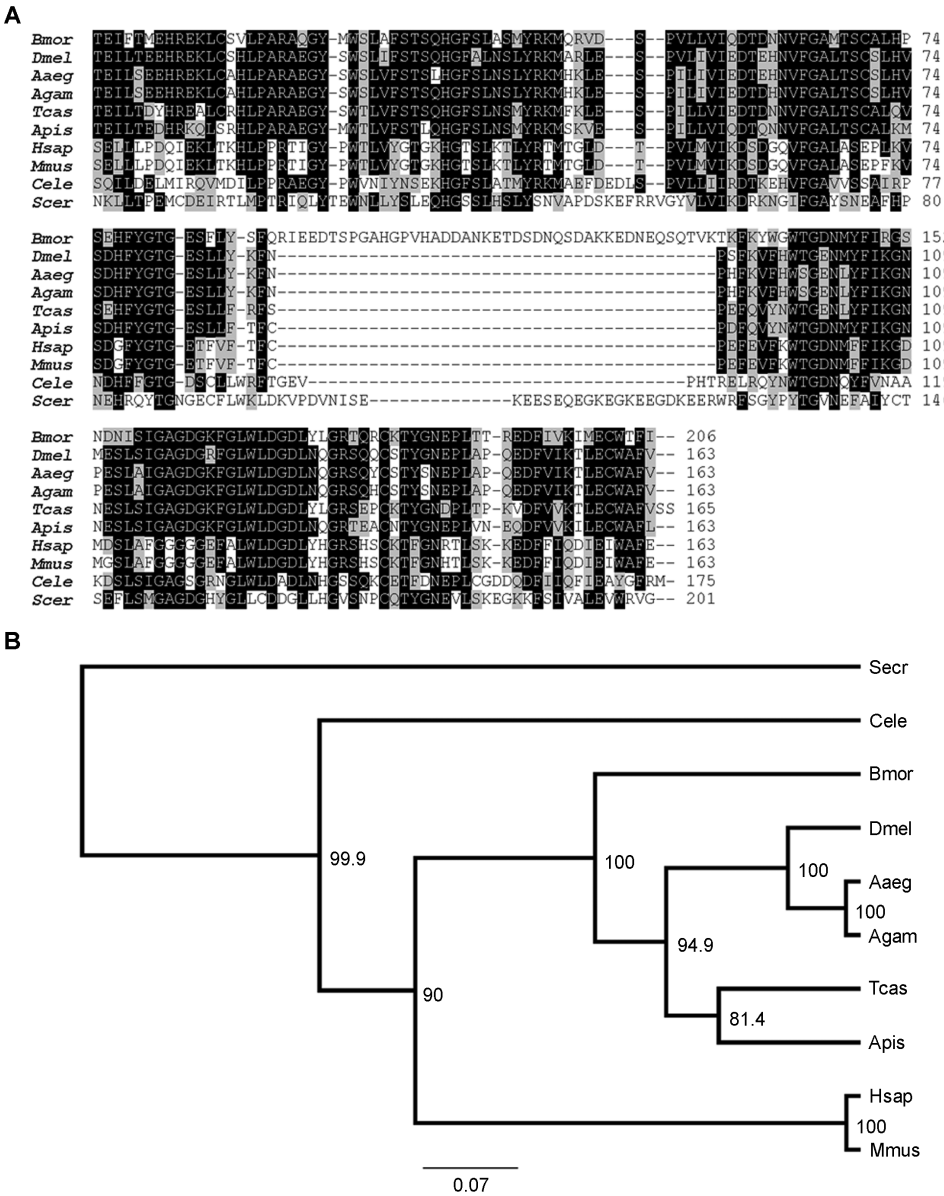

Fig. 2 Sequence comparison (A) and phylogenetic analysis (B) of TLDc domains. Aaeg, *Aedes aegypti* (XP_001662202.1); Agam, *Anopheles gambiae* (XP_003435918.1); Apis, *Acyrthosiphon pisum* (CYPI002835-PA); Bmor, *bombyx mori* (AK387280); Cele, *Caenorhabditis elegans* (CCD70813.1); Dmel, *Drosophila melanogaster* (Q9VNA1); Hsap, *Homo sapiens* (Q8N573.2); Mmus, *Mus musculus* (AAH98491.1); Scer, *Saccharomyces cerevisiae* (NP_015128.1); Tcas, *Tribolium castaneum* (XP_967175). The numbers on the tree branches represent bootstrap values for 1000 replicates.

Next we examined *BmOXR1* expression after injection of H_2O_2 (Fig. 3B). At high dosages of H_2O_2, variant A was up-regulated slightly at 3 h post-injection. At 6 and 12 h post-injection, variants A and D were induced strongly by H_2O_2. This result suggests that variants A and D might play major roles in the antioxidization process in larval silkworm.

The JNK inhibitor alters BmOXR1 expression induced by bacterial infection and H_2O_2

A study in mosquitoes revealed that the JNK pathway regulates *OXR1* expression (Jaramillo-Gutierrez *et al.*, 2010). To confirm that the same mechanism exists in silkworms, we examined *BmOXR1* expression induced

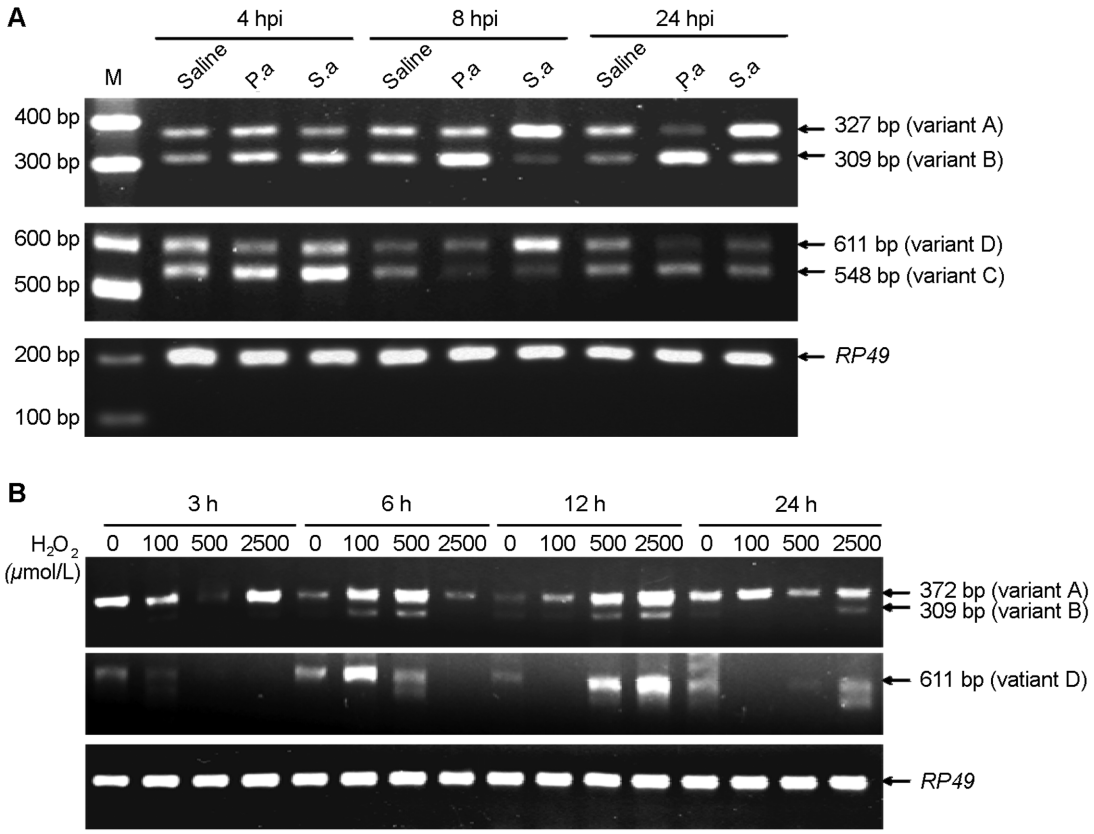

Fig. 3 Transcriptional profiles of different variants of *BmOXR1* gene after challenge by bacteria (A) and H_2O_2 (B). M, DNA ladder; Saline sterilized 0.9% NaCl as control; P.a, *Pseudomonas aeruginosa*; S.a, *Staphylococcus aureus*. Only one representative result from at least three independent experiments is shown here.

by bacteria and H_2O_2 after the administration of the JNK inhibitor SP600125. During *P. aeruginosa* infection, SP600125 down-regulated *BmOXR1* expression, except for transcript D (611 bp), which was increased at 8 hpi (Fig. 4A). Upon *S. aureus* infection, all four *BmOXR1* transcripts were down-regulated by SP600125 (Fig. 4B). Under H_2O_2 stress, the expression levels of variants A and D were also decreased after administration of SP600125 (Fig. 4C). Therefore, our results suggest that the JNK pathway is also involved in the regulation of *OXR1* expression in silkworm.

Larval silkworm survival and bacterial load are affected by JNK inhibitors

H_2O_2 is involved in insect defense (Ha *et al.*, 2005; Oliveira *et al.*, 2011; Diaz-Albiter *et al.*, 2011; Mikonranta *et al.*, 2014; Zhang & Lu, 2015a; 2015b). We showed above that the JNK inhibitor SP600125 modulated *BmOXR1* expression under bacterial infection and H_2O_2 stress. Therefore, we next investigated the effect of SP600125 on the survival of larval silkworms and the bacterial load in silkworms after infection. Administration of SP600125 decreased silkworm mortality after infection with both *S. aureus* and *P. aeruginosa* (Fig. 5A). CFU counts indicated that administration of SP600125 had no significant effect on *P. aeruginosa* growth in the hemolymph (Fig. 5B), while it slightly retarded the propagation of *S. aureus* inside the silkworm at an early stage of infection (Fig. 5C). Additionally, an interesting observation was that the level of *S. aureus* in the hemolymph was lower than that of *P. aeruginosa*, even though we injected the same amount of each.

Administration of a JNK inhibitor results in a higher level of H_2O_2 in the hemolymph during bacterial infection

To determine the reason the JNK inhibitor had effects on silkworm survival and bacterial growth during

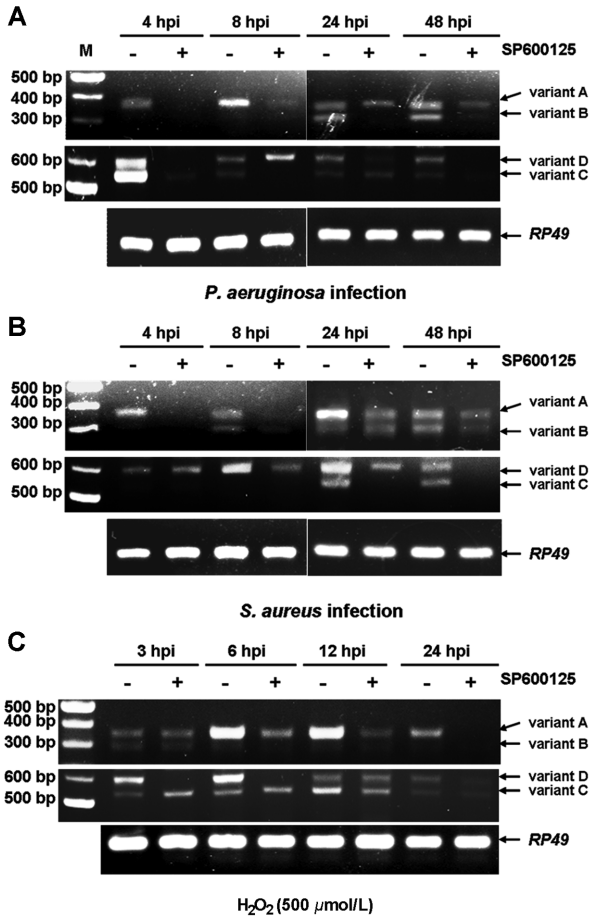

Fig. 4 Transcriptional profiles of *BmOXR1* gene during bacterial infection (A and B) and oxidative stress (500 μmol/L H_2O_2, C) are altered by Jun kinase (JNK) inhibitor SP600125.

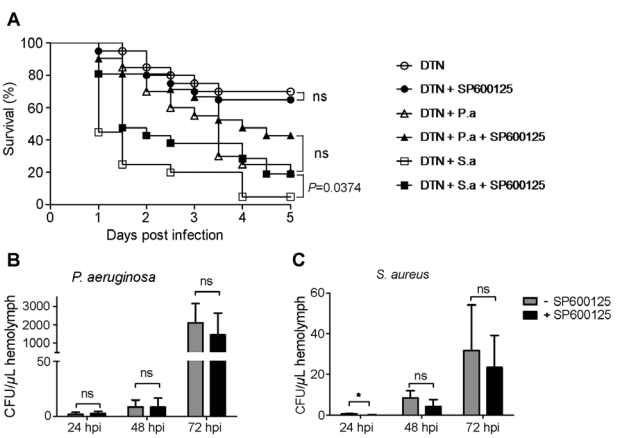

Fig. 5 Effects of administration of SP600125 on the survival of silkworm larvae (A) and viability of bacteria in the hemolymph (B and C). DTN, 10% dimethyl sulfoxide, 1.5% Tween-20 and 0.85% NaCl used to dissolve SP600125.

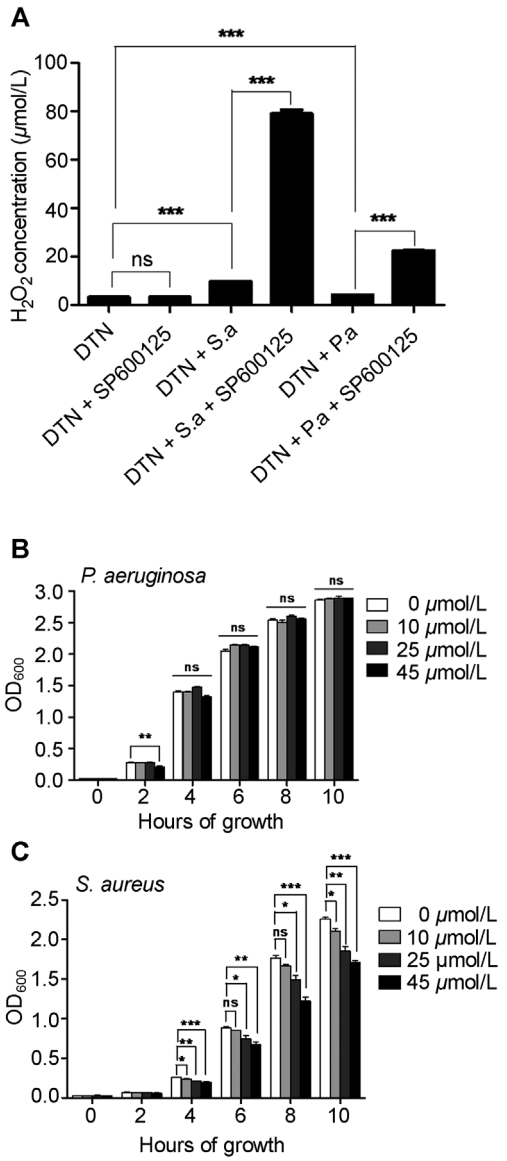

Fig. 6 Effects of administration of SP600125 on H_2O_2 concentration in the hemolymph (A) and sensitivity of *Pseudomonas aeruginosa* (B) and *Staphylococcus aureus* (C) to H_2O_2.

infection, we measured hemolymph H_2O_2 concentrations and *BmOXR1* expression levels after injection of SP600125 into infected larvae. First, the H_2O_2 concentrations in hemolymph increased significantly after bacterial infection and the levels of H_2O_2 increased much more after infection with *S. aureus* than with *P. aeruginosa* (Fig. 6A). Because SP600125 increased H_2O_2 levels in the hemolymph of both *S. aureus*- and *P. aeruginosa*-infected larvae and inhibited growth of both bacteria, yet the load

of *S. aureus* was significantly lower compared with *P. aeruginosa* (Fig. 5B and 5C), we speculated that the two bacteria might differ in their sensitivity to H_2O_2. Our assays indeed showed that *S. aureus* is susceptible to H_2O_2, whereas *P. aeruginosa* is not (Fig. 6B and 6C). Taken together, these results suggest that *BmOXR1* modulates hemolymph H_2O_2 levels through the JNK pathway in the silkworm during bacterial infection.

Discussion

Host insects produce ROS to combat invading microbes, such as bacteria (Ha *et al.*, 2005; Zhang & Lu, 2015a; Zhang & Lu, 2015b), viruses (Pan *et al.*, 2012; Wong *et al.*, 2015) and parasites (Surachetpong *et al.*, 2011; Andrews *et al.*, 2012; Diaz-Albiter *et al.*, 2011; Gonçalves *et al.*, 2012). In our previous study (Zhang & Lu, 2015a) and this study (Fig. 6A), we showed that H_2O_2 levels in larval silkworm hemolymph increased in response to bacterial infection. Furthermore, the bacterial load in hemolymph for the H_2O_2-sensitive bacterium *S. aureus* was slightly lowered at 24 h post-infection when we increased the H_2O_2 level using SP600125. The lower bacterial load consequently resulted in lower mortality of silkworm larvae (Fig. 5A).

However, we should bear in mind that the effects of ROS are highly dependent on its concentration. A moderate level of ROS is able to kill dangerous invaders (see above). On the other hand, a higher level of ROS is detrimental to the host. For instance, adult fruit flies with severely reduced immune-regulated catalase expression showed higher mortality rates after oral infection (Ha *et al.*, 2005). Likewise, depletion of catalase in the phlebotomine sand fly *Lutzomyia longipalpis* led to significantly increased mortality and a reduced number of developing oocytes after blood feeding (Diaz-Albiter *et al.*, 2011). In the pea aphid *Acyrthosiphon pisum*, after knocking down peroxiredoxin 1, a cysteine-based peroxidase, the elevation in H_2O_2 levels resulted in a reduction in bacterial numbers and an increase in aphid mortality after bacterial infection (Zhang & Lu, 2015b). Therefore, it is critical for the hosts to maintain homeostasis by elaborate regulation of ROS generation and elimination. In our current study, we did not observe any adverse effects on silkworm larval survival when the H_2O_2 level increased after SP600125 administration (Figs. 6A and 5A). This might be due to a relatively higher tolerance to ROS in larval silkworms. When Ishii *et al.* (2008) injected silkworm larvae with 50 μL of 100 mmol/L H_2O_2, harmful effects in the larvae were not observed. Based on these findings, we believe that administration of antioxidant agents would be helpful for silkworms to defend themselves against bacterial infection without causing oxidative stress under certain circumstances.

OXR1 has been shown to play roles as an antioxidant regulator (Volkert *et al.*, 2000; Elliott & Volkert, 2004; Oliver *et al.*, 2011; Sanada *et al.*, 2014; Liu *et al.*, 2015). In this study, we also showed that H_2O_2 induced expression of specific transcripts of OXR1 in larval silkworms (Fig. 3B). However, it is still unclear how OXR1 works as an antioxidant protein. Oliver *et al.* (2011) demonstrated that the C-terminal TLDc domain of mouse OXR1 alone was able to confer protection against oxidative stress by means of direct reaction with H_2O_2 through a conserved cysteine residue. In contrast, Murphy and Vokert (2012) believe the TLDc domain plays roles other than as an antioxidant, and they provided evidence that the human OXR1 exon 8 (corresponding to exon 17 of BmOXR1, see Fig. 1 and Fig. S2) is responsible for the prevention of oxidative damage. A study of nematode LMD-3, a homolog of human OXR1, showed that in addition to the TLDc domain, the N-terminal region also plays a role in defense against oxidative damage (Sanada *et al.*, 2014). Therefore, more biochemical investigations are needed to clarify OXR1 structure and function.

Although there is evidence supporting that OXR1 by itself is capable of preventing oxidative damage (discussed above), there is also evidence showing that OXR1 confers protection from oxidative stress by regulating the expression of ROS detoxification enzymes. *Anopheles gambiae OXR1* is regulated by the JNK pathway, and OXR1, in turn, regulates catalase and glutathione peroxidase genes (Jaramillo-Gutierrez *et al.*, 2010). Human OXR1 prevents oxidative stress by upregulating glutathione peroxidase-2 and heme oxygenase-1 expression, partly via the p21-Nrf2 signaling pathway (Yang *et al.*, 2014). A recent study showed that mouse OXR1 is regulated by microRNA-200b (Murray *et al.*, 2013). Our results (Fig. 4 and 6A) suggest that *BmOXR1* is regulated by the JNK pathway, as it is in mosquitoes. However, how the JNK pathway regulates OXR1 and whether other pathways are involved in OXR1 regulation require further investigation.

Acknowledgments

This study was financially supported by the National Natural Science Foundation of China (No. 31272497).

Disclosure

The authors declare no conflict of interest.

References

Andrews, E.S., Crain, P.R., Fu, Y., Howe, D.K. and Dobson, S.L. (2012) Reactive oxygen species production and *Brugia pahangi* survivorship in *Aedes polynesiensis* with artificial *Wolbachia* infection types, *PLoS Pathogens* 8, e1003075.

Blaise, M., Alsarraf, H.M.A.B., Wong, J.E.M.M., Midtgaard, S.R., Laroche, F., Schack, L., Spaink, H., Stougaard, J. and Thirup, S. (2012) Crystal structure of the TLDc domain of oxidation resistance protein 2 from zebrafish. *Proteins: Structure, Function, and Bioinformatics*, 80, 1694–1698.

Brandt, S.M., Jaramillo-Gutierrez, G., Kumar, S., Barillas-Mury, C. and Schneider, D.S. (2008) Use of a *Drosophila* model to identify genes regulating *Plasmodium* growth in the mosquito. *Genetics*, 180, 1671–1678.

Diaz-Albiter, H., Mitford, R., Genta, F.A., Sant'Anna, M.R.V. and Dillon, R.J. (2011) Reactive oxygen species scavenging by catalase is important for female *Lutzomyia longipalpis* fecundity and mortality. *PLoS ONE*, 6(3): e17486.

Diaz-Albiter, H., Sant'Anna, M.R.V., Genta, F.A. and Dillon, R.J. (2012) Reactive Oxygen species-mediated immunity against *Leishmania mexicana* and *Serratia marcescens* in the phlebotomine sand fly *Lutzomyia longipalpis*. *Journal of Biological Chemistry*, 287, 23995–24003.

Elliott, N.A. and Volkert, M.R. (2004) Stress induction and mitochondrial localization of Oxr1 proteins in yeast and humans. *Molecular and Cellular Biology*, 24, 3180–3187.

Gonçalves, R.L.S., Oliveira, J.H.M., Oliveira, G.A., Andersen, J.F., Oliveira, M.F., Oliveira, P.L. and Barillas-Mury, C. (2012) Mitochondrial reactive oxygen species modulate mosquito susceptibility to *Plasmodium* infection. *PLoS ONE*, 7: e41083.

Ha, E.M., Oh, C.T., Ryu, J.H., Bae, Y.S., Kang, S.W., Jang, I.H., Brey, P.T. and Lee, W.J. (2005) An antioxidant system required for host protection against gut infection in *Drosophila melanogaster*. *Developmental Cell*, 8, 125–132.

Ishii, K., Hamamoto, H., Kamimura, M. and Sekimizu, K. (2008) Activation of the silkworm cytokine by bacterial and fungal cell wall components via a reactive oxygen species-triggered mechanism. *Journal of Biological Chemistry*, 283, 2185–2191.

Jaramillo-Gutierrez, G., Molina-Cruz, A., Kumar, S., and Barillas-Mury, C. (2010) The *Anopheles gambiae* oxidation resistance 1 (OXR1) gene regulates expression of enzymes that detoxify reactive oxygen species. *PLoS ONE*, 5: e11168.

Kobayashi, N., Takahashi, M., Kihara, S., Niimi, T., Yamashita, O. and Yaginuma, T. (2014) Cloning of cDNA encoding a *Bombyx mori* homolog of human oxidation resistance 1 (OXR1) protein from diapause eggs, and analyses of its expression and function. *Journal of Insect Physiology*, 68, 58–68.

Liu, K.X., Edwards, B., Lee, S., Finelli, M.J., Davies, B., Davies, K.E. and Oliver, P.L. (2015) Neuron-specific antioxidant OXR1 extends survival of a mouse model of amyotrophic lateral sclerosis. *Brain*, 138, 1167–1181.

Mikonranta, L., Mappes, J., Kaukoniitty, M. and Freitak, D. (2014) Insect immunity: oral exposure to a bacterial pathogen elicits free radical response and protects from a recurring infection. *Frontiers in Zoology*, 11, 23.

Murphy, K. and Volkert, M. (2012) Structural/functional analysis of the human OXR1 protein: identification of exon 8 as the anti-oxidant encoding function, *BMC Molecular Biology*, 13, 26.

Murray, A.R., Chen, Q., Takahashi, Y., Zhou, K.K., Park, K. and Ma, J.X. (2013) MicroRNA-200b downregulates oxidation resistance 1 (Oxr1) expression in the retina of type 1 diabetes model. *Investigative Ophthalmology & Visual Science* 54, 1689–1697.

Nappi, A.J. and Ottaviani, E. (2000) Cytotoxicity and cytotoxic molecules in invertebrates. *BioEssays*, 22, 469–480.

Oliveira, J.H.M., Gonçalves, R.L.S., Lara, F.A., Dias, F.A., Gandara, A.C.P., Menna-Barreto, R.F.S., Edwards, M.C., Laurindo, F.R.M., Silva-Neto, M.A.C., Sorgine, M.H.F. and Oliveira, P.L. (2011) Blood meal-derived heme decreases ROS levels in the midgut of *Aedes aegypti* and allows proliferation of intestinal microbiota. *PLoS Pathogens*, 7: e1001320.

Oliver, P.L., Finelli, M.J., Edwards, B., Bitoun, E., Butts, D.L., Becker, E.B.E., Cheeseman, M.T., Davies, B. and Davies, K.E. (2011) Oxr1 is essential for protection against oxidative stress-induced neurodegeneration. *PLoS Genetics*, 7: e1002338.

Pan, X.L., Zhou, G.L., Wu, J.H., Bian, G.W., Lu, P., Raikhel, A.S. and Xi, Z.Y. (2012) *Wolbachia* induces reactive oxygen species (ROS)-dependent activation of the Toll pathway to control dengue virus in the mosquito *Aedes aegypti*. *Proceedings of the National Academy of Sciences of the United States of America*, 109, E23–E31.

Sanada, Y., Asai, S., Ikemoto, A., Moriwaki, T., Nakamura, N., Miyaji, M. and Zhang-Akiyama, Q.M. (2014) Oxidation resistance 1 is essential for protection against oxidative stress and participates in the regulation of aging in *Caenorhabditis elegans*. *Free Radical Research*, 48, 919–928.

Stowers, R.S., Russell, S. and Garza, D. (1999) The 82F late puff contains the *L82* gene, an essential member of a novel gene family. *Developmental Biology*, 213, 116–130.

Surachetpong, W., Pakpour, N., Cheung, K.W. and Luckhart, S. (2011) Reactive oxygen species-dependent cell signaling regulates the mosquito immune response to *Plasmodium falciparum*. *Antioxidants & Redox Signaling*, 14, 943–955.

Volkert, M.R., Elliott, N.A. and Housman, D.E. (2000) Functional genomics reveals a family of eukaryotic oxidation protection genes. *Proceedings of the National Academy*

of Sciences of the United States of America, 97, 14530–14535.

Wang, Z.P., Berkey, C.D. and Watnick, P.I. (2012) The *Drosophila* protein mustard tailors the innate immune response activated by the immune deficiency pathway. *The Journal of Immunology*, 188, 3993–4000.

Wang, Z.P., Hang, S.Y., Purdy, A.E. and Watnick, P.I. (2013) Mutations in the IMD pathway and mustard counter *Vibrio cholerae* suppression of intestinal stem cell division in *Drosophila*. *MBio*, 4(3), e00337–13.

Wong, Z.S., Brownlie, J.C. and Johnson, K.N. (2015) Oxidative stress correlates with *Wolbachia*-mediated antiviral protection in *Wolbachia–Drosophila* associations. *Applied and Environmental Microbiology*, 81, 3001–3005.

Yang, M., Luna, L., Sørbø, J.G., Alseth, I., Johansen, R.F., Backe, P.H., Danbolt, N.C., Eide, L. and Bjørås, M. (2014) Human OXR1 maintains mitochondrial DNA integrity and counteracts hydrogen peroxide-induced oxidative stress by regulating antioxidant pathways involving p21. *Free Radical Biology and Medicine*, 77, 41–48.

Zhang, L. and Lu, Z.Q. (2015a) Expression, purification and characterization of an atypical 2-Cys peroxiredoxin from the silkworm, *Bombyx mori*. *Insect Molecular Biology*, 24, 203–212.

Zhang, Y.D. and Lu, Z.Q. (2015b) Peroxiredoxin 1 protects the pea aphid *Acyrthosiphon pisum* from oxidative stress induced by *Micrococcus luteus* infection. *Journal of Invertebrate Pathology*, 127, 115–121.

Accepted September 9, 2015

Supporting Information

Additional Supporting Information may be found in the online version of this article at the publisher's web-site:

Figure S1. Comparison of the first six exons of OXR1 variants. Exons 1 to 6 are boxed with purple, yellow, gray, green, red and blue colors, respectively. "ATG" are highlighted with red color. Primers used for PCR detection are in bold and italicized.

Figure S2. Sequence comparison of BmOXR1 exon 8 with human OXR1 exon 17.